12-2012

Synthesis and CO2/CH4 separation performance of Bio-MOF-1 membranes.

Joseph Allen Bohrman 1988-
University of Louisville

SYNTHESIS AND CO_2/CH_4 SEPARATION PEFORMANCE OF BIO-MOF-1 MEMBRANES

By

Joseph Allen Bohrman
B.S. Ch.E., University of Louisville, May 2011

A Thesis
Submitted to the Faculty of the
University of Louisville
J. B. Speed School of Engineering
as Partial Fulfillment of the Requirements
for the Professional Degree

MASTER OF ENGINEERING

Department of Chemical Engineering

December 2012

SYNTHESIS AND CO_2/CH_4 SEPARATION PEFORMANCE OF BIO-MOF-1 MEMBRANES

Submitted by: _____
Joseph Bohrman

A Thesis Approved On

_____
(Date)

by the Following Reading and Examination Committee:

_____
Dr. Moises Carreon, Thesis Director

_____
Dr. Yongsheng Lian

_____
Dr. Gerold Willing

_____
Dr. James Watters

ACKNOWLEDGEMENTS

I cannot express how much gratitude and praise I have for Dr. Moises A. Carreon, my advisor. His continuous support and guidance helped me reach this milestone. Without his understanding, incredible knowledge, and most importantly, his friendship, I would not have been here today.

I would like to thank also my family and friends for their moral support when I wanted to throw in the towel. Their unyielding love gave me the motivation and drive I needed in continuing this journey.

I'd like to especially thank Minqi for her assistance in the lab. We started our research together and both grew into the students we are today. I will miss her friendship.

I give much gratitude towards Ms. Patricia Lumley and Dr. James Watters for their work in making this possible. My college career has been a twisted road that was kept straight with their much needed assistance.

Lastly, I would like to thank Dr. Yongsheng Lian and Dr. Willing for sitting on my thesis defense committee.

ABSTRACT

The separation of carbon dioxide from natural gas is of great interest from the environmental and energy perspective, respectively. From the environmental point of view, capturing CO_2 effectively from power plants can have a positive impact on reducing greenhouse gas emissions. From the energy point of view, CO_2 is an undesirable impurity in natural gas wells, with concentrations as high as 70%. Membrane technology can play a major role in making natural gas purification processes economically feasible.

A novel membrane composed of Metal-organic-framework material $Zn_8(Ad)_4(BPDC)_6O$ $2Me2NH_2$ (Bio-MOF-1) was designed and created to effectively separate CO_2/CH_4 gas mixtures. The crystalline structure, composition, and textural properties of Bio-MOF-1 membranes were confirmed through x-ray diffractometry, CHN analysis, transmission electron microscopy, adsorption measurements and BET surface area.

A secondary seeded growth approach was employed to prepare these membranes on tubular stainless steel porous support. These membranes displayed high CO_2 permeances ($11.5x10^{-7}$ mol / m^2 s Pa) and moderate CO_2/CH_4 separation selectivities (1.2 -2.5). The observed selectivities are above the Knudsen selectivity and indicate that the separation is promoted by preferential CO_2 adsorption over CH_4. This preferential adsorption is attributed to the presence of adeninate amino basic sites present in the Bio-MOF-1 structure. The work demonstrated shows the feasibility of the development of a novel type of membrane that could be promising for diverse molecular gas separations.

TABLE OF CONTENTS

NOMENCLATURE

Ad	=	adenine
Å	=	angstrom
a.u.	=	arbitrary unit
atm	=	atmosphere
BPDC	=	4,4'- biphenyl dicarboxylic acid
BET	=	Brunauer Emmett Teller
CO_2	=	carbon dioxide
CHN	=	Carbon, Hydrogen, Nitrogen
^oC	=	Celsius
Cu	=	Copper
cm^3	=	cubic centimeter
DEA	=	diethanolamine
θ	=	diffraction angle (degree)
DMF	=	N'N - dimethylformamide
d	=	d-spacing (Angstrom)
GC-MS	=	gas chromatograph – mass spectrometry
T_g	=	glass transition temperature (Celcius)
g	=	gram
hr	=	hour
H_2S	=	hydrogen sulfide
n	=	integer
Kα	=	K-alpha x-rays
K	=	kelvin
KPa	=	kilopascal
kV	=	kilovolt
P/P_o	=	measured pressure / saturation pressure
Mg	=	megagram
MW	=	megawatt
Bio-MOF	=	metal-biomolecule framework
MOF	=	metal-organic framework
CH_4	=	methane
MDEA	=	methyldiethanolamine
µm	=	micrometer
mA	=	milliamp
mL	=	milliliter
mmol	=	millimole
MMBtu	=	million metric british thermal units
MMT	=	million metric ton
min	=	minute

MEA	=	monoethanolamine
HNO_3	=	nitric acid
PPM	=	parts per million
Pa	=	pascal
PEI	=	polyethlenimine
P_i	=	permeance of species *i* (mol / m^2 s Pa)
RPM	=	revolutions per minute
SEM	=	scanning electron microscopy
s	=	second
m^2	=	square meter
TR	=	thermally rearranged
TGA	=	thermogravimetric analysis
TEM	=	transition electron microscopy
H_2O	=	water
λ	=	wavelength (Å)
XRD	=	x-ray diffractometry
$Zn(O_2CCH_3)_2(H_2O)_2$	=	zinc acetate dehydrate
Zn_4O	=	zinc oxide clusters
ZnO_4	=	zinc oxide tetrahedra

LIST OF TABLES

LIST OF FIGURES

I. INTRODUCTION

A. Environmental and Energy Concerns for Carbon Dioxide

1. Greenhouse Gas Emissions and a Rising Concern

Since the industrial revolution, human involvement has been increasingly adding to the amount of carbon dioxide in the atmosphere from 280 to 360 PPM[1]. In the past 250 years, the atmospheric level of carbon dioxide has risen by around 31%[2]. Carbon dioxide contributes to 60% of the greenhouse gases that cause global warming[1]. Figure 1 shows the distribution of CO_2 emissions among different US sectors by fuel source. In 2000 alone, CO_2 emissions accounted for 83% of total U.S. greenhouse gas emissions[3].

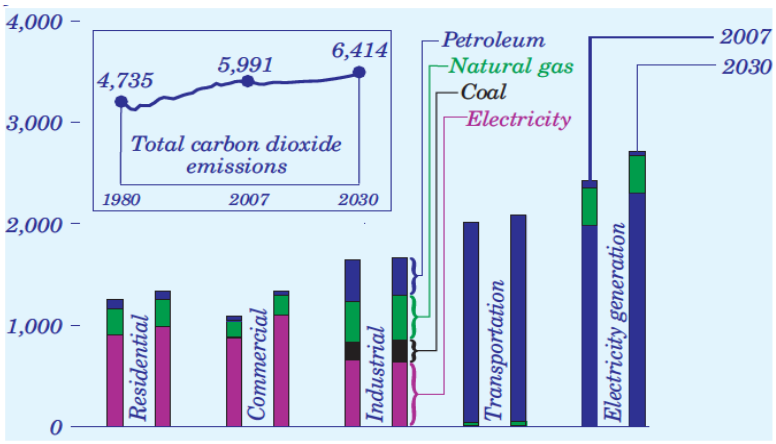

FIGURE 1 – CO_2 Emissions in the US by sector and fuel (in MMT)[32]

As these gases, especially CO_2, continue to increase, potential adverse effects on regional and global climate, ecosystem function, and human health increase as well. In an effort to reduce these emissions, many national governments are looking to introduce mandatory reporting of greenhouse gas emissions. As recently as July 2009, a 1,200 page

climate-change and energy bill (H.R. 2454) made its way through Congress in order to establish a "cap and trade" system to reduce carbon dioxide emissions[4]. The bill would cut emissions by 17% of 2005 levels by 2020 and by 83% of 2005 levels by 2050[4]. Reporting emissions using thresholds is also part of efforts in the EU and Canada to monitor greenhouse gas emissions. The Ontario Ministry of the Environment (MOE) currently has a mandatory emissions monitoring and reporting program that requires facilities to report if emissions exceed 100,000 Mg of CO_2[5]. Although steps around the globe have been initiated to quell the situation, world energy-related CO_2 emissions will increase by approximately 40% by 2040 according to current projected rates[4].

2. Natural Gas as an Alternative Fuel Source and Associated Challenges

Coinciding with the growing concern of atmospheric CO_2 concentrations is world energy demands. Fossil fuels account for approximately 80% of the worldwide energy demand which produces CO_2[6]. In an effort to reduce fossil fuel energy production, research is being directed towards alternative fuels, carbon capture, and carbon sequestration. With the emergence of these new technologies, estimates suggest that U.S. natural gas reserves have doubled and gas prices have dropped from a high of $15/MMBtu in 2006 to less than $3/MMBtu in early 2012[7]. Low costs combined with an abundance of supply makes natural gas combustion turbines look extremely attractive for electricity generation. U.S. power generation from natural gas grew from 14% in 1997 to 23% in 2010[7]. Natural gas power plants provide many advantages including higher efficiency and lower sulfur and CO_2 emissions per MW generated[7]. If CO_2 emissions become heavily regulated, a shift towards natural gas power plants will accelerate in the future.

In order to effectively use natural gas as a fuel source, the fuel supply must be purified of any impurities to increase its energy content. Carbon dioxide is an undesirable impurity in natural gas wells, with concentrations as high as 70%[8]. In addition to lowering the energy content of natural gas, carbon dioxide is acidic and corrosive in the presence of H_2O. Current pipeline specifications require a CO_2 concentration below 2-3%[9].

3. Current Separation Methods and a Shift to Green Technologies

The most widely used process to purify natural gas utilizes alkanolamine aqueous solution to absorb selectively CO_2 and H_2S from natural gas streams[10]. The most commonly used amines in industrial plants are the alkanolamines monoethanolamine (MEA), diethanolamine (DEA), and methyldiethanolamine (MDEA), all of which are harmful to the environment and human health[11]. This process is extremely energy intensive and requires multiple steps in preparation for the separation and solution recovery (heating of the solution, recovery of acid gases, etc.). Figure 2 displays a common schematic for an alkanolamine treating process for natural gas purification.

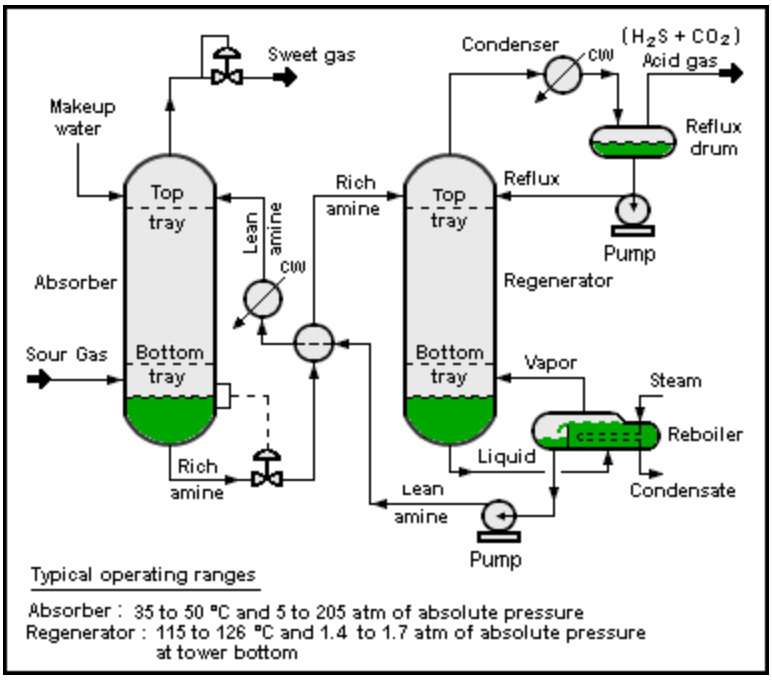

FIGURE 2 – Process Flow Diagram of Natural Gas Alkanolamine Treatment[11]

In an effort to reduce the high energy consumption, chemicals involved, phase changes, complex equipment, and proneness to pollution, membrane technology is being increasingly adopted in the industry[12]. Rather than subject the feed gas stream to multiple steps, a simple, pressure driven design would promote the separation of CO_2 from CH_4.

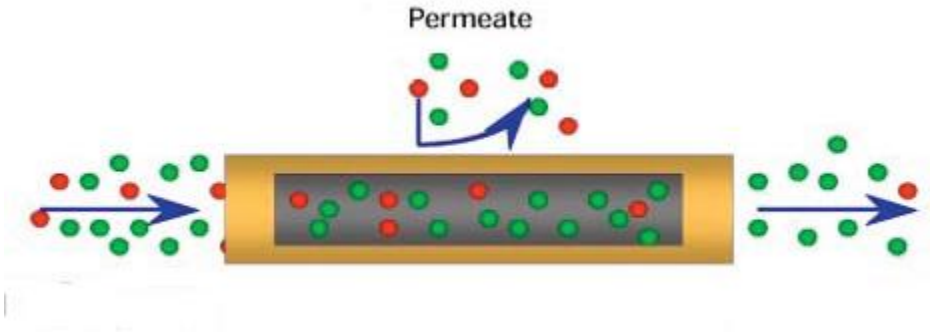

FIGURE 3 – Conventional Membrane Technology for Gas Separation[13]

Figure 3 shows this technology where a gaseous mixture (in this case CO_2/CH_4) would enter the tubular support from the left and the CO_2 would permeate through the walls while the remaining CH_4 would exit the support. Polymeric membranes have been

the industry standard for separation because of their competitive performance as well as their low manufacturing/production costs[14]. For gaseous separations, nonporous membranes are used. The vapors and gases are separated by their difference in solubility and diffusivity in the polymers[15]. Small molecules move among the polymer chains according to the formation of local gaps by thermal motion of polymer segments. Porous membranes rely solely on the Knudsen diffusion for the separation of gaseous mixtures[15].

B. Gaseous Mixture Separations Utilizing Nanoporous Material Membranes

1. What are Metal-Organic Frameworks?

While polymeric membranes are highly sought after for their low manufacturing/production costs and high performance, they do have weaknesses. Plasticization is a common occurrence for polymeric membranes. With the sorption of CO_2, polymers swell and change in mechanical and physical properties. The most important of these is the reduction of the glass transition temperature (T_g), simply called plasticization[16]. The CO_2 molecules interact with the basic site within the polymer and reduce chain-chain interactions. This reduction increases the mobility of polymer segments thus reducing the glass transition temperature (T_g). Plasticization causes thermal instability and can lead to fracturing of the polymeric membrane[16]. Materials that are able to withstand harsh conditions (thermally and chemically stable) while able to adsorb large amounts of CO_2 (high surface areas) are needed for the purification of natural gas.

A family of materials that are able to provide each of these characteristics is metal-organic frameworks (MOFs). MOFs are crystalline compounds consisting of metal

ions or clusters coordinated to often rigid organic molecules to form three-dimensional porous structures. Figure 4 displays the prototypical metal-organic framework MOF-5[20].

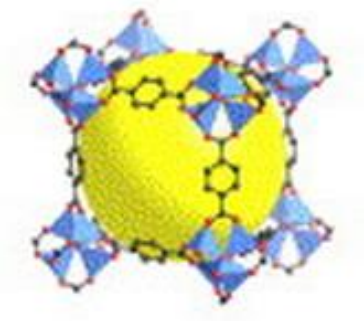

FIGURE 4 - Cubic Topology of MOF-5[17]

MOF-5 is built up by Zn_4O groups on the corners of a cubic lattice, interconnected by terephthalic acid ligands. ZnO_4 tetrahedra (polyherda) are joined by benzene dicarboxylate linkers (O and C) creating pore apertures of 8 Angstroms and a 12 Angstrom pore diameter (sphere). MOF-5 has thermal stability up to 400°C and a high surface area of 2900 m^2g^{-1} [18]. Compared to zeolites, another family of well-known materials used in the separation of gaseous mixtures, MOFs have a much larger diversity in porosity allowing for a broad range of applications such catalysis (large pore diameter/volume) and especially gas separations (small pore diameter/volume). Figure 5 compares several MOFS (dots and squares) to a few zeolites (diamonds) to visually display the diversity within this family of materials.

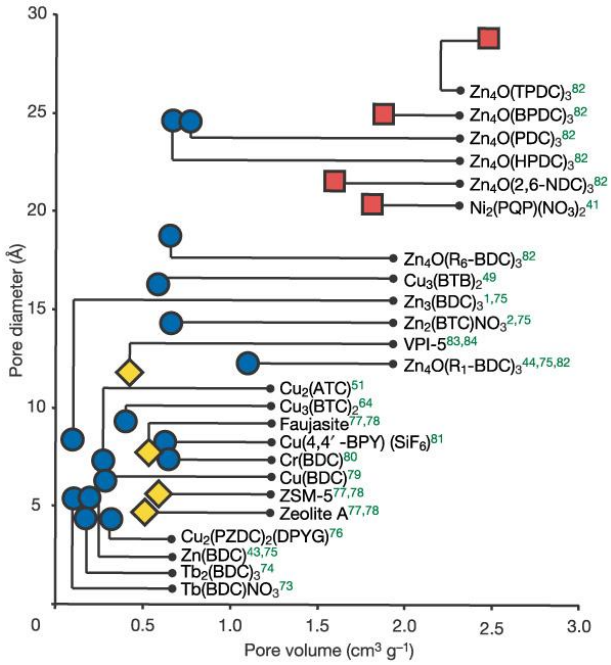

FIGURE 5 – Porosity of MOFS Compared to Zeolites[19]

2. How do MOFs differ from Bio-MOFs?

The ability of MOFs to be carefully tailored, coupled with their diverse applications, makes them one of the most growing areas of research. New generations of MOFS are being designed to be compatible with the environment and human body[20]. To accomplish this task, biomolecules are incorporated in the construction of MOFs as ligands, as opposed to traditional organic ligand (imidazole, etc.). This subset of materials in the MOF family is known as Bio-MOFs. With the introduction of biomolecules as ligands, additional advantages are introduced such as structural diversity (rigid or flexible) which impacts the functional nature of the Bio-MOF, as well as high CO_2 adsorption capacity[20].

The biomolecules available for the construction of Bio-MOFs can be categorized within one of five groups: amino acids, peptides, proteins, nucleobases, and saccharides (carbohydrates). Each group of biomolecules provides excellent ligands. However,

nucleobases (key constituent of nucleic acids which is involved in base-pairing) make the ideal bio-linkers[20]. Nucleobases have H-bonding capabilities and multiple nitrogen electron lone pairs which allows for rich binding sites (multidentate). Of the wide range of nucleobases existing, adenine (Figure 6) has been the most reported[20]. Adenine offers five binding sites, each located at an amino group.

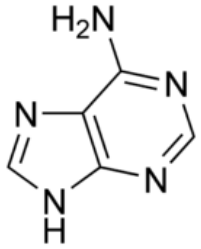

FIGURE 6 – Adenine Molecule Displaying Multiple Binding Sites[21]

3. Background and Research on Bio-MOF-1

The first three-dimensional permanently porous framework using adenine to derive a Bio-MOF was $Zn_8(Ad)_4(BPDC)_6O{\cdot}2(NH_2(CH_3)_2)+$, 8 DMF, 11 H_2O, also known as Bio-MOF-1[20]. Bio-MOF-1 consists of Zn(II)-Adeninate column composed of octahedral cages with each cage consisting of 8 Zn^{2+} cations with 4 adeninate linkers, Figure 7[22].

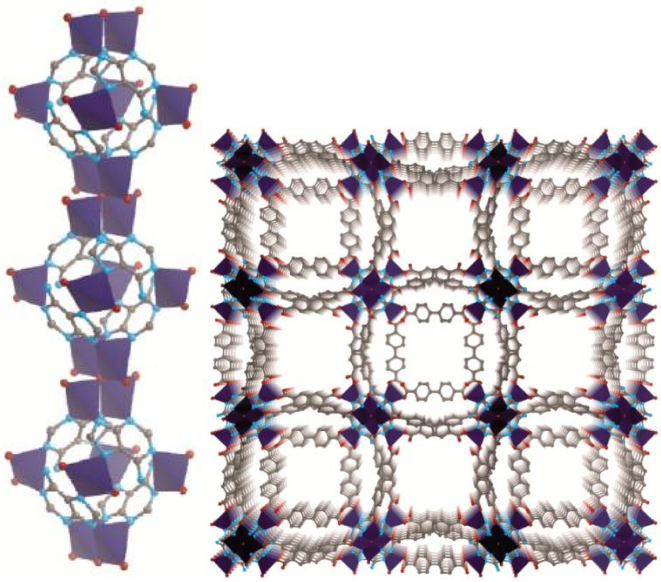

FIGURE 7 – Structural Features of Bio-MOF-1, Columns (Left) and Framework (Right)[22]

Each column is interconnected via biphenyldicarboxlyate forming a tetragonal lattice crystal system with pore apertures of approximately 5.2 Angstroms. Nitrogen adsorption studies revealed that Bio-MOF-1 has a BET surface area of 1700 m^2 g^{-1}. Thermogravimetric analysis (TGA) revealed a decomposition temperature of approximately 300^oC[22].

C. Justification

Bio-MOF-1 possesses some highly appealing properties that are necessary for the separation of CO_2 from CH_4 in an effort to purifying natural gas wells. The biomolecule adenine used as a ligand provides rich binding sites for carbon dioxide adsorption. Other promising properties of Bio-MOF-1 include high surface area, thermal stability, and chemical stability.

D. Objectives

The objectives of the current study are to:

1) Develop Bio-MOF-1 crystals displaying narrow size distribution and enhanced CO_2 adsorption properties.
2) Develop reproducible and continuous Bio-MOF-1 membranes for CO_2/CH_4 separation.
3) Establish basic structure/separation relationships of Bio-MOF-1 membranes in relevant functional gas separations related to natural gas.

II. EXPERIMENTATION

A. Synthesis of Bio-MOF-1

The zinc-adeninate metal-organic framework Bio-MOF-1 was synthesized similarly to the method described by Rosi's group[22]. In a typical synthesis, shown in Figure 8, 0.25mmol of Adenine ($C_5H_5N_5$, Sigma Aldrich Inc., ≥99.0%), 0.5mmol of 4,4'-biphenyl dicarboxylic acid (BPDC, $HO_2CC_6H_4C_6H_4CO_2H$, Sigma Aldrich Inc., 97%), and 0.75mmol of zinc acetate dihydrate ($Zn(O_2CCH_3)_2(H_2O)_2$, Sigma Aldrich Inc., ≥99%) were dissolved in a mixture of 2mmol of nitric acid (HNO_3, Sigma Aldrich Inc., ≥90.0%), 2mL of deionized water, and 13.5mL of N,N-dimethylformamide (DMF, $HCON(CH_3)_2$, Acros Organics, 99.8%). To facilitate the disolution, the solution was vigorously stirred for 30 minutes at 300 RPM. The prepared gel solution was poured into a 50 mL Teflon vessel. Each vessel was placed into an autoclave to allow the solution to reach an autogenous pressure as heated. The autoclave was placed into a programmable oven with a 1^oC/min ramp up from room temperature to 130°C for 24 hours.

Rod-shaped colorless crystals obtained after synthesis were separated from the effluent by centrifugation at 3000 RPM and washed three times with 3mL of DMF. The resulting crystals were then placed in a Precision vacuum oven and subjected to drying in an argon atmosphere at a temperature of 125 °C for 2 hours.

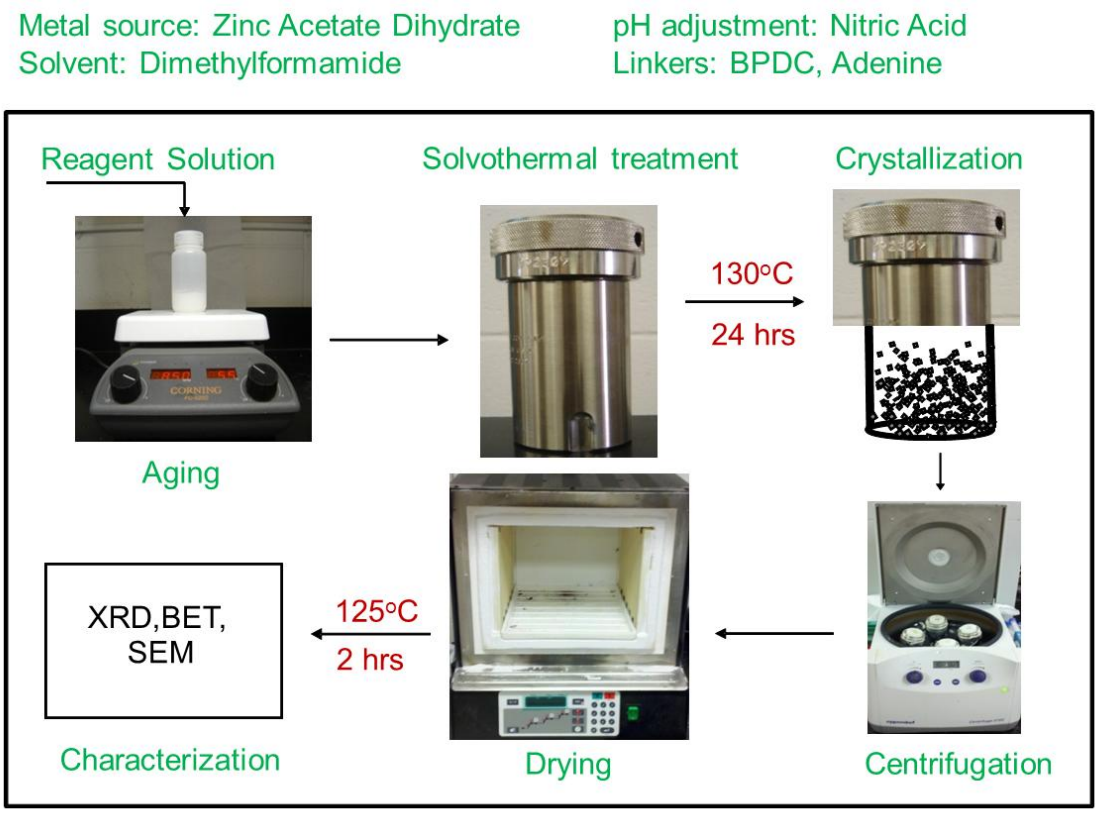

FIGURE 8 – Bio-MOF-1 Crystal Synthesis

B. Bio-MOF-1 Characterization

The resulting crystals were then characterized using X-ray diffraction, scanning electron microscopy, transmission electron microscopy, CHN analysis and BET surface area. The powder X-ray diffraction patterns were gathered by use of the Bruker D8-Discover diffractometer, Figure 15, at 40 kV, 40 mA with Cu Kα radiation. The BET surface area measurements were taken on a Micromeritics Tristar 3000 porosimeter which operated at 77 K using liquid nitrogen as coolant. The samples were degassed at 130 °C for three hours directly before being placed in the porosimeter. The scanning electron microscopy was performed using a FE-SEM (FEI Nova 600) with an

acceleration voltage of 6 kV. The quantitative analysis of elemental carbon, hydrogen, and nitrogen were carried out at Midwest Microlab, LLC (Indianapolis).

C. Bio-MOF-1 Membrane Preparation and Testing

Bio-MOF-1 membranes were prepared via secondary seeded growth inside tubular porous stainless steel supports (0.1 grade, 0.27 μm pores, Mott Corporation), Figure 9. The synthesis solution preparation and composition is similar to that use for the synthesis of Bio-MOF-1 seeds. The membranes were prepared by rubbing the inside surface of porous supports with dry Bio-MOF-1 seeds using cotton swabs. The rubbed porous supports, with their outside wrapped in Teflon tape, were then placed vertically in a 50mL Teflon autoclave and filled with the synthesis solution. The reaction was carried out at the same conditions for seed synthesis (130^{o}C for 24 hours) in the Ney® Vulcan 3-550 Furnace. The resulting membranes were gently washed with DMF not only to rinse the membrane, but also remove excess buildup of crystals within the tubular support. Multiple layers were applied following the same procedure. The membranes were dried at 100^{o}C under an argon atmosphere within the Precision Vacuum Oven.

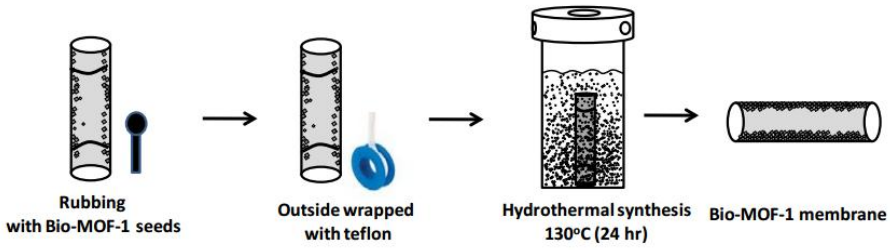

FIGURE 9 – Bio-MOF-1 Membrane Synthesis

The separation performance of the Bio-MOF-1 membranes for equimolar CO_2/CH_4 gas mixture was measured in a separation system shown in Figure 10. The membranes were mounted in a stainless steel module with silicone O-rings as seals on

both ends. The driving force across the membrane was provided by a pressure drop of 138 KPa with the permeate pressure being 99.5 KPa (atmospheric). The permeate gas rate was measured by a soap film bubble flow meter. The total flow rate was 100 mL/min. The compositions of the feed, retentate, and permeate streams were measured using a gas chromatograph (SRI instruments, 8610C) equipped with a thermal conductivity detector and HAYESEP-D packed column, Figure 19. The oven, injector and detector temperatures in the GC were kept at 65°C, 100°C and 150°C respectively.

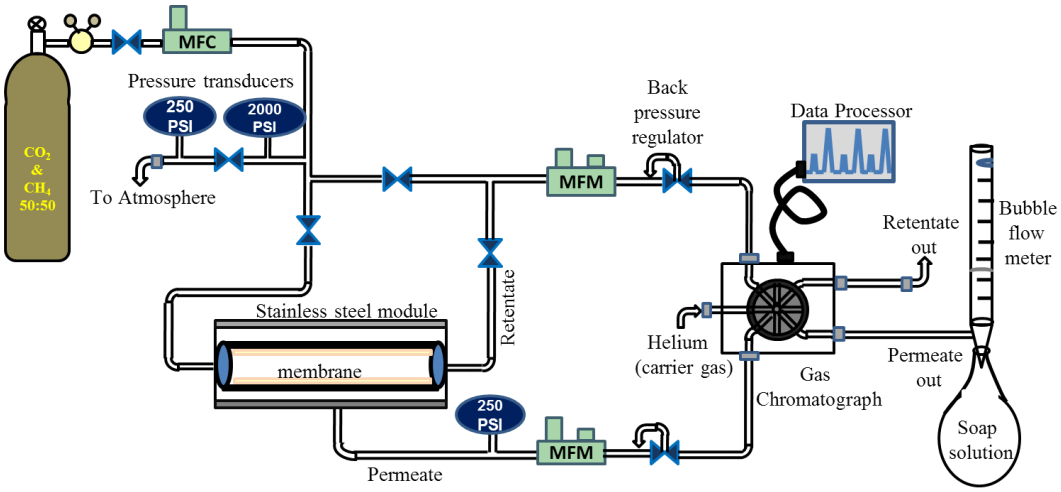

FIGURE 10 – Gas Separation System Schematic

E. Equipment

1. Synthesis of Bio-MOF-1

FIGURE 11 - Hydrothermal Autoclave with 50mL Teflon Vessel

FIGURE 12 - Ney® Vulcan 3-550 Furnace
Dentsupply Ceramco International
Serial No.: 9493308
York, PA 17404

FIGURE 13 - Eppendorf Centrifuge
Model No: 5702
Serial No: 5702YN320989

FIGURE 14 - Precision Vacuum Oven
Model No.: 29
Serial No.: 69902505
Winchester, VA 22602

2. Bio-MOF-1 Characterization

FIGURE 15 - X-Ray Diffraction,
Bruker AXS – Diffraktometer D8
Serial No.: 203407
Karlsruhe, Germany D76181[23]

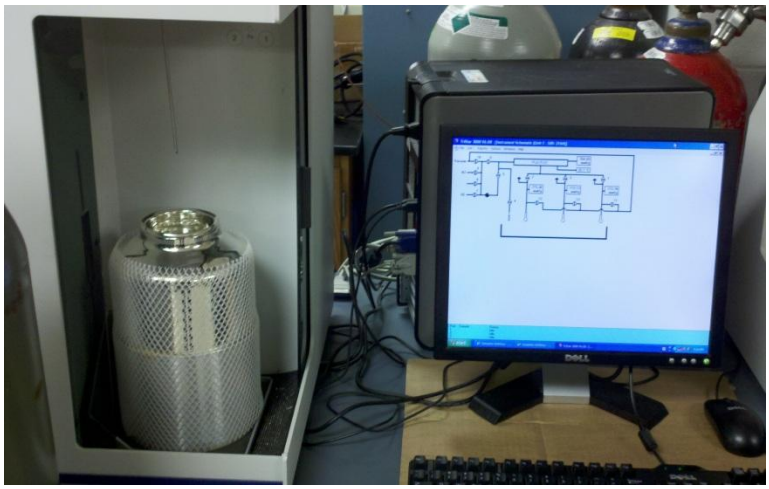

FIGURE 16 - Micromeritics Tristar 3000 Porosimeter

FIGURE 17 - Nova NanoSEM 600
FEI[24]

3. Bio-MOF-1 Membrane Testing

FIGURE 18 - Stainless Steel High Pressure Gas Separation System
Model No: 4576A

FIGURE 19 - GC-MS
HP 5890 Gas Chromatograph equipped with 5970 Mass Selective Detector

III. RESULTS AND DISCUSSION

A. Characterization of Bio-MOF-1

The method provided by Rosi was followed closely to create Bio-MOF-1[22]. Several samples were successfully created using this method, each of approximately 0.1 g of product. This yielded the correct crystalline structure, with the powder X-ray diffraction pattern matching closely that shown in Figure 20. The relative intensity and peak positions of the XRD pattern are in agreement with the typical structure of Bio-MOF-1[22]. Some of the secondary peaks were broader and less intense than the reported XRD pattern of Bio-MOF-1 from Rosi's group, indicating that although the Bio-MOF-1 crystals maintained long-range cystallinity, its framework may have a greater degree of local structural disorder. Local structural distortions have been associated with surface relation effects and/or the presence of extended structural defects[25].

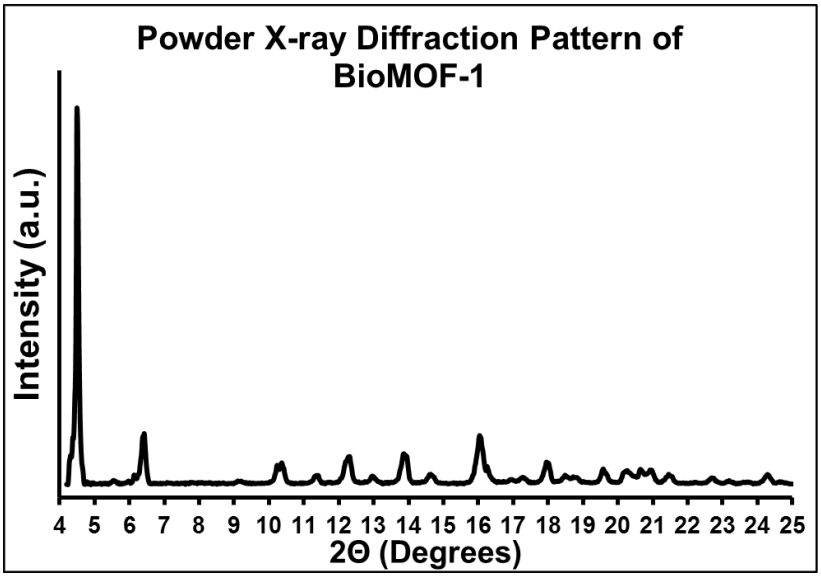

FIGURE 20 – XRD Pattern of Bio-MOF-1[26]

Scanning electron microscopy images of Bio-MOF-1 crystals can be seen in Figure 21. The sample shown on the left displays two phases, a nanobar crystalline phase and an amorphous spherical phase. The presence of the amorphous Bio-MOF-1 phase suggests that the necessary synthesis reaction time had not been met. The sample on the right displays well-defined nanobars with lengths ranging from 0.5-4.5 μm and widths from 0.05-0.15 μm were observed[26]. The uniform surface morphology and crystal size suggests that membrane formation is possible due to excellent packing. Excellent packing is imperative in membrane formation in the reduction in nonselective pathways.

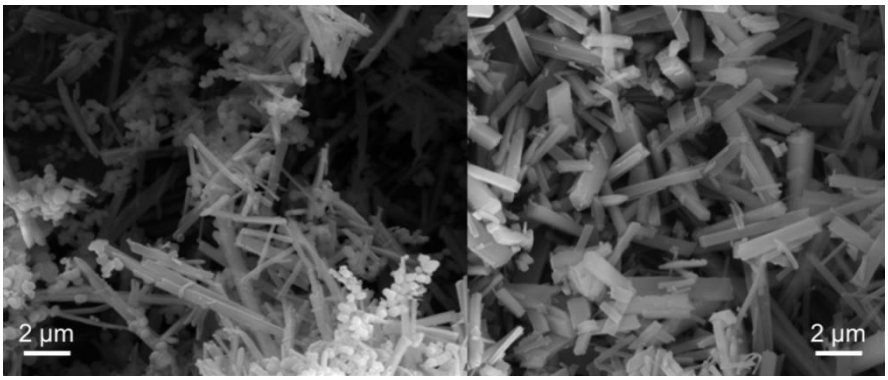

FIGURE 21 – SEM surface morphology of two phase Bio-MOF-1 crystals (Left) and pure nanobar Bio-MOF-1 crystals (Right)[26]

The apparent BET surface area of the Bio-MOF-1 crystals was approximately 800 $m^2 g^{-1}$. While this value is much lower than previous reports[22, 20], the lower surface area may be related to the incomplete removal of dimethylammonium cations, DMF or to water residing in the pores of the structure and/or to the extent of local disorder in the framework as noted from the XRD pattern inconsistencies[26]. Attempts to remove these molecules by solvent exchange (chloroform, methanol, etc.) resulted in the framework collapsing. Other varying drying methods were attempted in opening the Bio-MOF-1 framework such as under vacuum (20 inHG) and at varying temperatures, however, all attempts again led to the framework collapsing.

CHN analysis revealed that the carbon, hydrogen, and nitrogen contents of the Bio-MOF-1 framework were C-46.6%, H-3.9%, and N-11.7%[26], which agree with the calculated theoretical amounts of C-46.7%, H-4.7%, and N-12.3%[22]. The adsorption isotherms at low P/P_o relative pressure of CO_2 and CH_4 for Bio-MOF-1 were collected at room temperature. Figure 22 shows that Bio-MOF-1 crystals preferentially adsorbed CO_2 over CH_4. At P/P_o approximately 0.04, the crystals adsorbed 9 times more CO_2 than CH_4 reaffirming their appealing nature for CO_2 separation from other gases[26]. This preferential

adsorption can be attributed to the presence of adeninate amino basic sites within the porous framework[26].

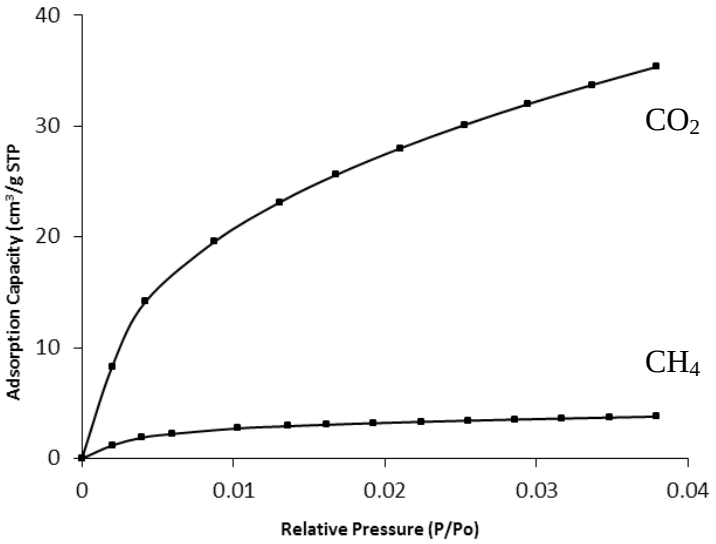

FIGURE 22 – Bio-MOF-1 CO2 and CH4 adsorption capacities[26]

Transmission electron microscopy (TEM) was employed as an additional means of characterizing the synthesized seeds. Figure 23 shows the TEM images of two nanobars selected from the crystalline sample shown in Figure 21. Below each TEM images is the visual diffraction pattern presenting the spacing between particular crystal planes.

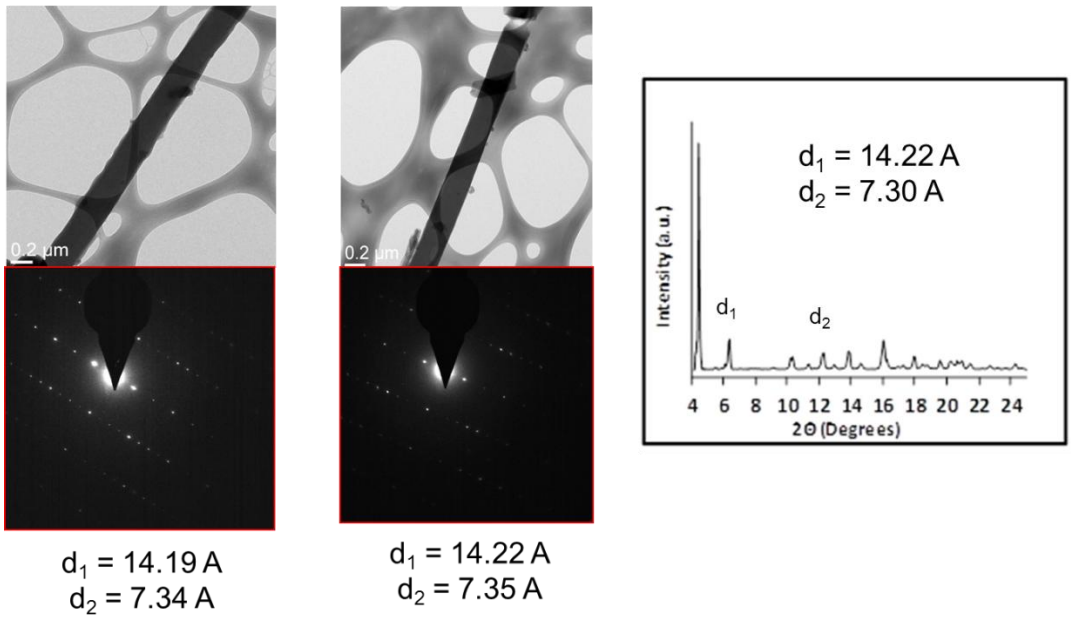

FIGURE 23 – TEM and Diffraction Patterns (Left) and XRD Pattern (Right) for Bio-MOF-1 Seeds

Utilizing Bragg's law[27], the d-spacings calculated agree well with those found through the TEM analysis as indicated in the XRD pattern in Figure 23.

$$n\lambda = 2dsin\Theta$$

Where n is an integer, λ is the wavelength of the incident wave, d is the spacing between the planes in the atomic lattice, and Θ is the angle between the incident ray and the scattering planes.

B. Membrane Separation Performance

As described in Bio-MOF-1 membrane preparation and testing, the secondary seeded growth approach was employed to prepare the membranes. This method provides nucleation sites for membrane growth as well as eliminates gaps in between the particles through the addition of multiple layers. Elimination occurs either through attachment of newly formed crystals or by the growth of the crystals already present on the

membrane[26]. Figure 24 presents SEM images obtained of the top view as well as the cross section.

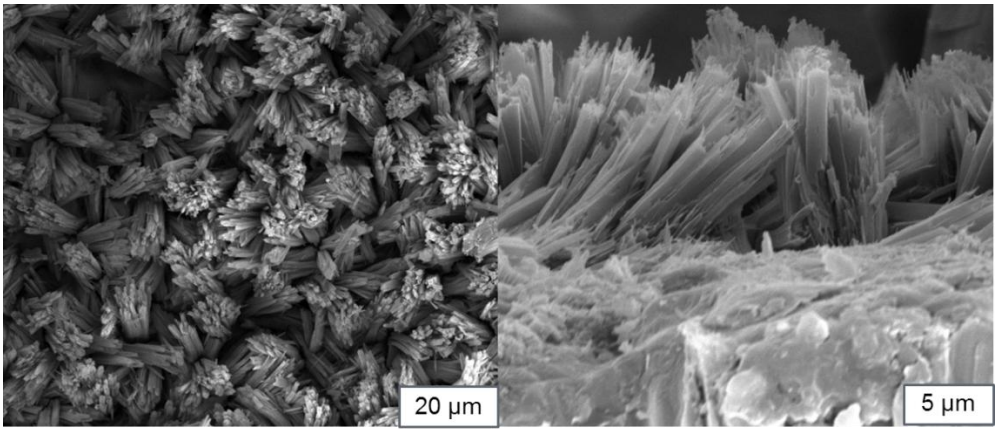

FIGURE 24 – SEM images of Bio-MOF-1 Membrane Surface Morphology: Top view (Left) and Cross-Section (Right)[26]

The Bio-MOF-1 membrane surface and cross sectional views display the same nanobar crystal morphology as seen previously in the synthesized seeds (Figure 21). Lengths in the ~ 9-11 µm range and widths in the ~ 1-2 µm range were observed. The increase in size is related to the recrystallization and growth of the crystals with the incorporation of multiple layers[26]. The preferential perpendicular growth direction suggests an epitaxial growth mechanism[26]. The thickness of this particular membrane was ~15 µm. The XRD pattern of the membrane corresponds to the structure of Bio-MOF-1, Figure 25.

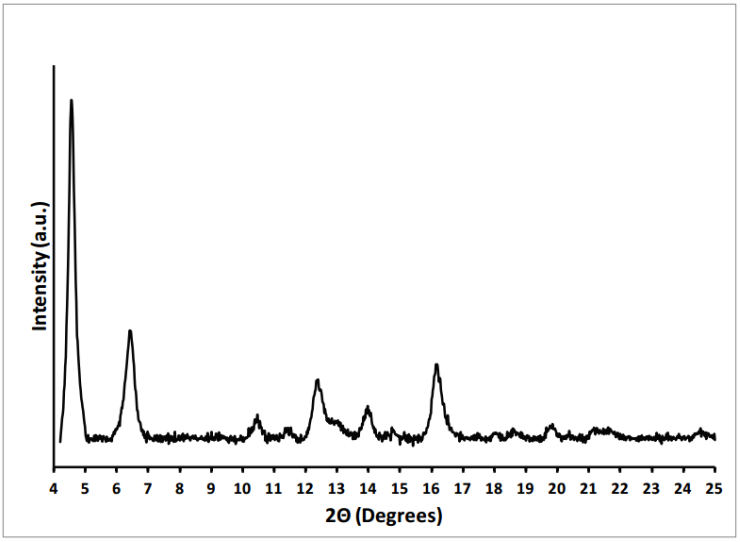

FIGURE 25 – XRD Pattern of Bio-MOF-1 Membrane (M1)

The difference in peak intensity, between the main peak and secondary peaks, as compared to the XRD pattern of the seeds, Figure 20, may indicate the preferential orientation of the crystals. This behavior has been observed in other MOF films[28].

The CO_2/CH_4 separation performance of the stainless steel supported Bio-MOF-1 membranes is show in Table 1. At least 3 layers were needed to obtain continuous membranes. Membranes M1 and M2 were prepared with three layers, M3 with 4 layers, and M4 with 7 layers. CO_2 permeances as high as 11.9 x 10^{-7} $mol \cdot m^{-2}s^{-1}Pa^{-1}$ and CO_2/CH_4 selectivities of 2.6 were observed[26]. Membrane reproducibility was confirmed by the similar separation performances of M1 and M2. The addition of multiple layers correlated with a decrease in CO_2 permeance and CO_2/CH_4 selectivity.

TABLE I

CO_2/CH_4 SEPARATION PERFORMANCE OF BIO-MOF-1 MEMBRANES AT TRANS-MEMBRANE PRESSURE DROP OF 138 KPA AND 298K[26].

Membrane [a]	P_{CO2} ($x10^{-7}$) mol/m^2·s·Pa	P_{CH4} ($x10^{-7}$) mol/m^2·s·Pa	CO_2/CH_4 selectivity
M1 (3)	11.5	4.6	2.5
M2 (3)	11.9	4.6	2.6
M3 (4)	10.5	4.8	2.2
M4 (7)	5.8	4.7	1.2

a) Numbers in parenthesis indicate number of layers

The decrease in CO_2 permeance is due to an increase in membrane thickness. The addition of more layers results in an increase of Bio-MOF-1 pores (selective) and non-Bio-MOF-1 pores (non-selective)[26]. The selective transport pathways for CO_2 are a consequence of the basic adeninate sites. The non-selective pathways associate with intercrystalline boundaries and/or amorphous regions, since these pores differ in size and adsorption properties compared to the selective pathways. Therefore, the decrease in CO_2/CH_4 selectivity suggests the addition of more layers results in a higher concentration of non-selective pathways[26]. The observed CO_2/CH_4 selectivities are greater than 0.6 suggesting that the main mechanism of separation is preferential adsorption of CO_2 over CH_4 and not Knudsen selectivity[29]. Again, this is supported by Figure 22 which shows that the CO_2 adsorption capacities of Bio-MOF-1 crystals are higher than that of CH_4.

The Robeson plot for CO_2/CH_4 separation selectivities as a function of CO_2 permeabilities (permeance x membrane thickness) of polymeric membranes has been widely used to compare the performance of membranes[30]. For comparison, the separation performance for Bio-MOF-1 membrane M1 has been included in this plot, shown in Figure 26.

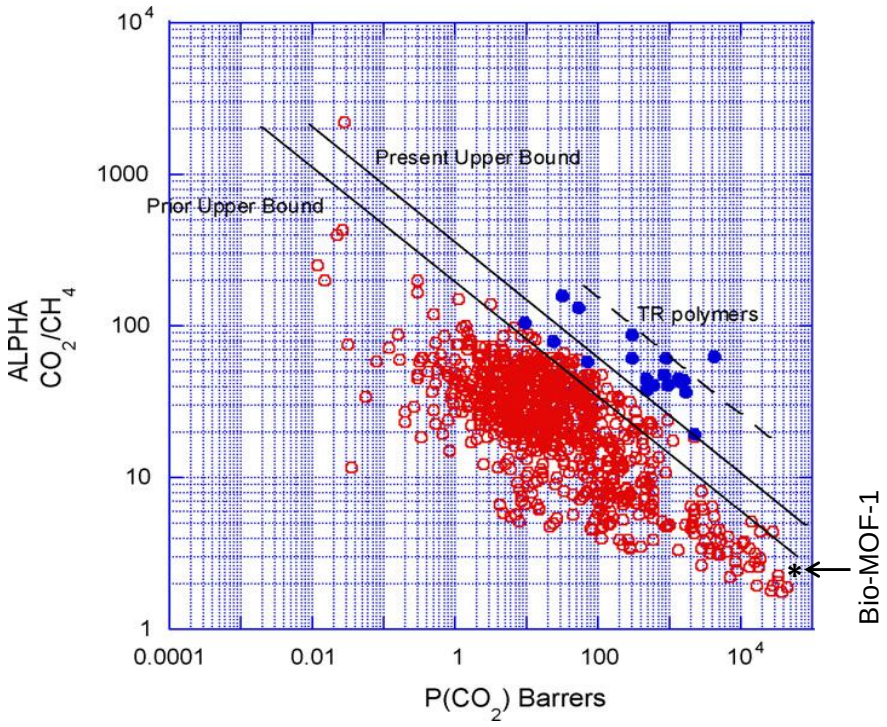

FIGURE 26 – Robeson Plot for CO_2/CH_4 Mixtures[30]

The data point for the Bio-MOF-1 membrane lies in the region of conventional polymeric membranes. Although its separation performance is lower than that of thermally rearranged (TR) polymeric membranes and most zeolitic membranes, it lies at the upper extremities for CO_2 permeances[31]. Further optimization of synthesis and processing parameters during the preparation of these membranes could potentially lead to more CO_2 selective membranes and ultimately extremely competitive and sought after membranes.

IV. CONCLUSIONS

Bio-MOF-1 crystals were developed following the presented methods by Rosi[22]. Comprehensive characterization techniques were used to study the textural and morphological properties of the generated Bio-MOF-1. TEM, CHN analysis, and XRD all confirmed the synthesized material was indeed Bio-MOF-1. Local structural disorder was observed from the obtained XRD patterns by noticing the broader and less intense secondary peaks. The crystals obtained displayed a BET surface area of ~800 m^2 g^{-1}. This value is only half of that reported[22] and can be attributed to dimethyl ammonium cations, DEF solvent, and water remaining within the framework. Further attempts (solvent exchange, vacuum drying, etc.) failed to vacate the Bio-MOF-1 pores. Scanning electron microscopy was also performed on the Bio-MOF-1 crystals, previously unreported. The SEM images reveal nanobar shaped particles of length ranging from 0.5-4.5 μm and width from 0.05-0.15 μm. Adsorption isotherms were acquired displaying CO_2 adsorbed 9 times more than CH_4 reaffirming their appealing nature for separation.

The preparation of continuous and reproducible Bio-MOF membranes was demonstrated for a functional gas mixture separation for the first time. The membranes were prepared via secondary seeded growth on tubular porous supports. At least 3 layers were needed to obtain continuous membranes. The reproducibility was confirmed by the similar separation performance of M1 and M2 membranes. These membranes displayed high CO_2 permeances (11.5 x 10^{-7} $mol \cdot m^{-2} s^{-1} Pa^{-1}$) and separation ability for CO_2/CH_4 gas mixtures. The observed CO_2/CH_4 selectivites (2.5-2.6) were above the Knudsen

selectivity indicating that the separation is promoted by preferential CO_2 adsorption over CH_4. This preferential CO_2 adsorption was attributed to the presence of adeninate amino basic sites in the Bio-MOF-1 structure. The addition of more layers resulted in a decrease in CO_2 permeance and CO_2/CH_4 selectivity. The decrease in separation performance was related to the increase in concentration of non-selective pathways. SEM images of the membrane revealed intergrown bunches of nanobar crystals covering the surface of the support. Lengths in the 9-11 μm range and widths in the 1-2 μm were observed. The increase in size and preferred growth direction suggest epitaxial growth.

V. RECOMMENDATIONS

A. Synthesis of Bio-MOF-1

Difficulties were encountered with repeatability in the synthesis of high surface area Bio-MOF-1. Various other chemicals could be utilized in the solvent exchange such as acetone, ethanol, and toluene in hopes of vacating the porous framework. Different Bio-MOF-1 compositions need to be explored as well as different parameters such as inorganic precursors, synthesis time, and treatment temperature. Each of these could result in the reduction in local structural disorder and thus increasing the stability of the framework for solvent removal.

B. Characterization of Bio-MOF-1

Additional characterization techniques can be used to investigate the Bio-MOF-1 crystal and membrane framework. It would also be helpful to run a comparative TGA on the crystals with respect to the published literature. The thermal stability of the crystals may have decreased due to the large amount of structural disorder, thus leading to the collapse of the framework during drying and drastically reducing the surface area.

C. Separation Performance of Bio-MOF-1

Future experiments of Bio-MOF-1 membrane synthesis should focus on employing different seeding techniques in an effort to prepare more robust, continuous membranes. The secondary seeded growth mechanism provides nucleation sites;

however, wherever there are vacancies located on the tubular support, the seeds cannot establish growth. By employing a method utilizing a PEI (polyethylenimine) solution, anchoring of Bio-MOF-1 seeds to the entire surface is possible removing the chance for non-selective pathways, invariably increasing the separation performance. As stated previously, several of the synthesis parameters (gel composition, treatment time and temperature) can be explored during membrane synthesis, coupled with seeding mechanisms, to increase the robust nature of the membrane.

REFERENCES CITED

1. Saha, D.; Bao, Z.; Jia, F.; Deng, S., Adsorption of CO_2, CH_4, N_2O, and N_2 on MOF-5, MOF-177, and Zeolite 5A. Environmental Science & Technology 2010, 44 (5), 1820-1826.
2. Srivastava, R.; Srinivas, D.; Ratnasamy, P., Zeolite-based organic-inorganic hybrid catalysts for phosgene-free and solvent-free synthesis of cyclic carbonates and carbamates at mild conditions utilizing CO_2. Appl. Catal., A 2005, 289, 128.
3. Gillenwater, M. Inventory of US Greenhouse Gas Emissions and Sinks: 1990-2000 US Environmental Protection Agency, Office of Atmospheric Programs. EPA 430-R-02-003, 2002.
4. Hogue, C.; Johnson, J., Cap & Trade: Razor thin House vote clears CO_2 Emissions Bill. Chem. Eng. News, 2009, 87 (27), 8.
5. Ontario Ministry of the Environment. Step by Step Guideline for Emission Calculation, Record Keeping and Reporting for Airborne Contaminant Discharge; Ontario Ministry of the Environment: Ontario, Canada, 2001 [available at http://www.ene.gov.on.ca/envision/monitoring/monitoring.htm].
6. Annual Energy Outlook 2007; Energy Information Agency Report No. DOE/EIA-0383; 2007
7. Cost and Performance Baseline for Fossil Energy Plants, Volume 1: Bituminous Coal and Natural Gas to Electricity; National Energy Technology Laboratory Report No. DOE/NETL-2010/1397; November 2010.
8. Lin, H., Van Wagner, E., Raharjo, R., Freeman, B. D. and Roman, I. (2006), High-Performance Polymer Membranes for Natural-Gas Sweetening. Adv. Mater., 18: 39–44.
9. Baker, Richard W. "Future directions of membrane gas separation technology."Industrial & Engineering Chemistry Research 41.6 (2002): 1393-1411.
10. Rochelle, Gary T. "Amine scrubbing for CO_2 capture." Science 325.5948 (2009): 1652-1654.
11. Kohl, Arthur L., and Richard B. Nielsen. Gas purification. Gulf Professional Publishing, 1997.
12. Bernardo, P., E. Drioli, and G. Golemme. "Membrane gas separation: a review/state of the art." Industrial & Engineering Chemistry Research 48.10 (2009): 4638-4663.
13. Untitled Membrane Image. n.d.Innovative Gas Systems, *IGS - Innovative Gas Systems*. Web. http://www.igs-global.com/images/gas-comp/Membrane-Separation-Gas.jpg
14. Perry, R.H., Green D.H., Perry's Chemical Engineers' Handbook,7th edition, McGraw-Hill, 1997.
15. Vieth W.R., Diffusion in and through Polymers, Hanser Verlag, Munich, 1991.
16. Kazarian, S. G. "Polymer processing with supercritical fluids." Polymer science series cc/c of Vysokomolekuliarynye Soedineniia (2000): 78-101.

17. Rowsell, Jesse LC, and Omar M. Yaghi. "Metal–organic frameworks: a new class of porous materials." Microporous and Mesoporous Materials 73.1 (2004): 3-14.
18. Z Botas, J. A.; Calleja, G.; Sánchez-Sánchez, M.; Orcajo, M. G., Cobalt Doping of the MOF-5 Framework and Its Effect on Gas-Adsorption Properties. Langmuir 2010, 26 (8), 5300-5303.
19. Yaghi, O.M.; O'Keeffe, M.; Ockwig, N.W.; Chae, H.K.; Eddaoudi, M.; Kim, J. Nature 2003, 423, 705-714.
20. Imaz, Inhar; Rubio-Martinez, Marta; An, Jihyun; Sole-Font, Isabel; Rosi, Nathaniel L.; Maspoch, Daniel. "Metal–biomolecule frameworks (MBioFs)." Chemical Communications 47.26 (2011): 7287-7302.
21. Adenine. 27 Dec. 2008. Pepemonbu. *Wikipedia*. Web. http://upload.wikimedia.org/wikipedia/commons/d/db/Adenine.svg
22. An, Jihyun, Steven J. Geib, and Nathaniel L. Rosi. "High and Selective CO_2 Uptake in a Cobalt Adeninate Metal− Organic Framework Exhibiting Pyrimidine-and Amino-Decorated Pores." Journal of the American Chemical Society 132.1 (2009): 38-
23. Chong, N. Synthesis and Characterization of Ceria Nanomaterials. University of Louisville, 2010
24. Manufacturer Specifications - Nova NanoSEM 600, FEI. http://www.medwow.com/med/scanning-electron-microscope/fei/nova-nanosem-600/33713.model-spec.
25. Petkov, Valeri, et al. "Structure of gold nanoparticles suspended in water studied by x-ray diffraction and computer simulations." Physical Review B 72.19 (2005): 195402.
26. Bohrman, Joseph A., and Moises A. Carreon. "Synthesis and CO2/CH4 separation performance of Bio-MOF-1 membranes." Chemical Communications(2012).
27. Tanaka, Shunsuke, et al. "Structure of mesoporous silica thin films prepared by contacting PEO106-PPO70-PEO106 films with vaporized TEOS." Chemistry of materials 18.23 (2006): 5461-5466.
28. Venna, Surendar R., Jacek B. Jasinski, and Moises A. Carreon. "Structural evolution of zeolitic imidazolate framework-8." Journal of the American Chemical Society 132.51 (2010): 18030-18033.
29. Poshusta, Joseph C., Richard D. Noble, and John L. Falconer. "Temperature and pressure effects on CO_2 and CH_4 permeation through MFI zeolite membranes." Journal of membrane science 160.1 (1999): 115-125.
30. Robeson, Lloyd M. "The upper bound revisited." Journal of Membrane Science 320.1 (2008): 390-400.
31. H.B. Park, C.H. Jung, Y.M. Lee, A.J. Hill, S.J. Pas, S.T. Mudie, E. Van Wagner, B.D. Freeman, D.J. Cookson, Polymers with cavities tuned for fast selective transport of small molecules and ions, Science. 318 (2007) 254-258.
32. Annual energy outlook 2009 with projections to 2030. Report #: DOE/EIA – 0383(2009)

Appendix

TABLE II

BET TABULAR RESULTS FOR BIO-MOF-1 SEEDS

Relative Pressure (P/Po)	Quantity Adsorbed (cm^3/g STP)	Relative Pressure (P/Po)	Quantity Adsorbed (cm^3/g STP)
0.085284884	101.0416346	0.988505632	202.4063994
0.141860462	104.0001233	0.973981437	196.6911398
0.201808211	106.2501795	0.958531702	189.8380122
0.241422118	107.5643403	0.940030582	183.6617938
0.299912856	109.2279586	0.924635831	179.6340394
0.349478361	110.5649683	0.906950282	175.4540002
0.447326429	112.9701176	0.876976432	169.8707106
0.546429907	115.5581823	0.842319976	165.0035217
0.645560837	118.8837421	0.803475779	159.910523
0.734648608	123.6798326	0.742813275	153.3590492
0.795036187	129.8059179	0.651920325	148.1732261
0.835832231	137.1362219	0.555455965	144.7931218
0.870030478	147.068239	0.447830418	119.6655654
0.900865679	158.8131435	0.348424522	116.1584689
0.922986443	167.4247847	0.224790326	112.7515423
0.937611403	173.1665736		
0.950916804	178.3030655		
0.961711466	182.9093868		
0.969500442	186.5590045		
0.975475075	189.9578135		
0.980606686	193.6100396		
0.983071645	196.0481408		
0.985545808	198.4882379		
0.987085227	200.4397495		
0.988505632	202.4063994		

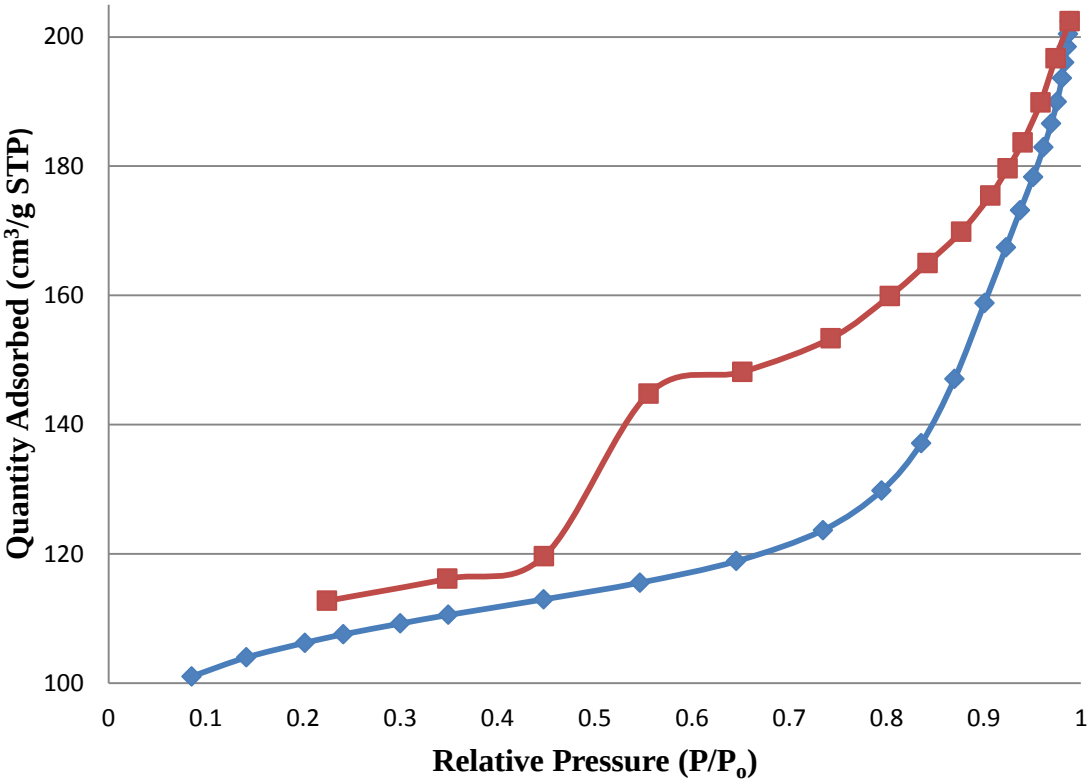

FIGURE 27 – BET Isotherms for Bio-MOF-1 Seeds

TABLE III

BET TABULAR RESULTS FOR BIO-MOF-1 MEMBRANE CRYSTALS

Relative Pressure (P/Po)	Quantity Adsorbed (cm^3/g STP)	Relative Pressure (P/Po)	Quantity Adsorbed (cm^3/g STP)
0.087852798	198.6660322	0.988338981	242.9892746
0.14363503	202.5710531	0.969738226	241.0465045
0.203083625	205.3480062	0.945568241	240.2291491
0.242925223	206.8653635	0.921298621	239.7563644
0.299893054	208.6339085	0.886827064	239.1664989
0.349428544	210.0313368	0.875060839	238.9382772
0.447333898	212.3701049	0.841326532	238.2232195
0.5463551	214.8314134	0.801514808	237.4051002
0.645386274	218.3524254	0.74230533	236.2066259
0.734584095	224.0874745	0.653486106	234.0497556
0.796981655	229.2355451	0.553677834	230.542763
0.837959044	232.3943754	0.450003981	214.7805157
0.872440614	234.9787888	0.351122259	212.1115687
0.902568437	237.2927268	0.224065469	208.5533649
0.923440695	238.4398766		
0.93846468	238.9318747		
0.951426445	239.369909		
0.962614722	239.9088276		
0.969947428	240.3326504		
0.975925209	240.8502315		
0.981046081	241.4252457		
0.98322796	241.7867135		
0.985230512	242.1786736		
0.987163304	242.6522096		
0.988338981	242.9892746		

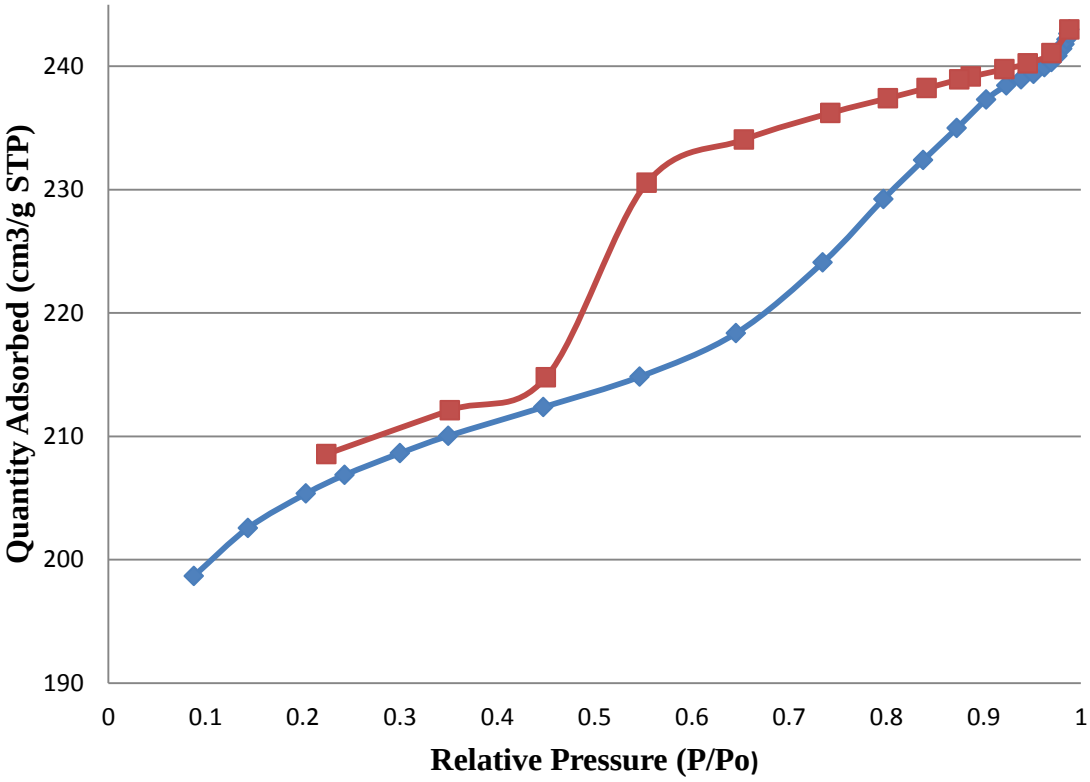

FIGURE 28 - BET Isotherms for Bio-MOF-1 Membrane Crystals

VITA

NAME: Joseph Bohrman

ADDRESS: Department of Chemical Engineering
University of Louisville
Louisville, KY 40292

DOB: Paducah, KY – February 14, 1988

EDUCATION & TRAINING:

B.S., Chemical Engineering
University of Louisville
2006-11

M.Eng., Chemical Engineering
University of Louisville
2011-12

HONORS & AWARDS:

Hallmark Scholarship, University of Louisville, 2006-2011

PROFESSIONAL SOCIETIES:

American Institute of Chemical Engineers

Tau Beta Pi Engineering Society

North American Membrane Society